4428 J. Phys. Chem. A **2004,** *108,* 4428−4432

Theoretical Study on the Reaction Mechanisms of C_2H with O_2

Laicai Li,*,[†] Ping Deng,[†] Anmin Tian,[‡] Minghou Xu,[§] and Ning-Bew Wong[||]

Department of Chemistry, Sichuan Normal University, Chengdu 610066, People's Republic of China, Faculty of Chemistry, Sichuan University, Chengdu 610064, People's Republic of China, State Key Laboratory of Coal Combustion, Huazhong University of Science and Technology, Wuhan 430074, People's Republic of China, and Department of Biology and Chemistry, City University of Hong Kong, Kowloon, Hong Kong

Received: December 1, 2003; In Final Form: March 17, 2004

The complicated microscopic reaction mechanism of the ethynyl radical with molecular oxygen has been investigated by systematically employing density functional theory and ab initio molecule orbital methods. Geometries and harmonic frequencies of reactants, intermediates, transition states, and products have been investigated at the MP2 with 6-31G(d) and 6-311++G(d,p) basis sets and B3LYP/6-311++G(d,p) theoretical levels, respectively. The QCISD(T) method with the 6-311++G(d,p) basis set has been used in the final single-point energy calculation. The present study reveals that, at room temperature, the main reaction pathways of the reaction of C_2H radical with molecule oxygen is $C_2H + O_2 \rightarrow M1 \rightarrow TS(1-2) \rightarrow M2 \rightarrow TS(2-3) \rightarrow M3 \rightarrow TS(3-P2) \rightarrow CH + CO_2$. At the same time, several other exothermic pathways have also been characterized.

1. Introduction

The ethynyl radical (C_2H) exists widely in nature and artificial environments.[1−4] Always being an important intermediate, C_2H has been the subject of numerous investigations. Vakhtin and co-workers[5] have studied the reactions of C_2H with ethylene, propylene, and 1-butylene in low-temperature conditions, and Look and Peeters[6] have investigated the reactions of C_2H radical with O_2, C_2H_2, and H_2O in the range of temperature of about 295−450 K through experiments. In the combustion processes, C_2H is formed by H atom abstraction from acetylene or by other reactions, e.g. $O + C_3H$. Obviously, the reaction of C_2H with O_2 plays an important role in this process, so many works have been devoted to studying it either in experiments or in theories.[6−18] There are many pathways for the reaction of C_2H with O_2 and different reaction products at different temperatures. Sumathi[19] pointed out there were five exothermic reaction pathways as follows:

$$C_2H + O_2 \rightarrow CO + HCO \qquad \Delta H^{19} = -151 \text{ kcal/mol}$$

$$\rightarrow CO + CO + H \qquad \Delta H^{19} = -136 \text{ kcal/mol}$$

$$\rightarrow CH + CO_2 \qquad \Delta H^{19} = -87 \text{ kcal/mol}$$

$$\rightarrow C_2O + OH \qquad \Delta H^{19} = -36 \text{ kcal/mol}$$

$$\rightarrow HCCO + O \qquad \Delta H^{19} = -33 \text{ kcal/mol}$$

As possible products of the above reactions, CH, CO, CO_2, and HCCO have been explored through experiments.[3−10] For the OH radical, there have been no experimental reports so far. So in the present study, we studied the microscopic mechanism of the five reaction channels in detail, employing quantum chemistry methods, and have tried to give a full picture of the complicated reaction process of C_2H with O_2 theoretically.

2. Computational Details

All calculations were performed with the GAUSSIAN 98 package of programs.[20] The geometries for all species were fully optimized employing the second-order Møller−Plesset perturbation method (MP2) with 6-31G(d) and 6-311++G(d,p) basis sets and density functional method (B3LYP) with the 6-311++G(d,p) basis set, respectively. The harmonic vibration frequencies were also obtained at the corresponding level in order to characterize the stationary points as local minima or first-order saddle points, to obtain zero-point vibration energy corrections (ZPE), and to generate force constant data needed in the intrinsic reaction coordinate (IRC) calculation. The IRC method was used to track minimum energy paths from transition structures to the corresponding local minima. A step size of 0.1 amu$^{1/2}$ bohr or larger was used in the IRC procedure. In addition, single point energies were calculated using the quadratic configuration interaction method, which includes the effect of single, double, and triple substitutions, QCISD(T). Again, the 6-311++G(d,p) basis set was used with this method. Restricted wave functions are used for closed-shell and unrestricted wave functions for open-shell systems with all orbitals active. For each species the degree of spin contamination was monitored. For doublet systems, the $\langle S^2 \rangle$ value did not exceed 0.78 and the $\langle S^2 \rangle$ values were not greater than 2.0 for triplets, thus indicating that the wave functions were not significantly contaminated by higher order spin states.

3. Results and Discussion

Analysis of Reaction Mechanism of C_2H with O_2. The equilibrium geometries of the various isomers and transition states are presented in Figure 1. As can be seen from the figure, the two intermediates, M1 and M5, are produced at the first

---

[†] Sichuan Normal Unversity.
[‡] Sichuan University.
[§] Huazhong University of Science and Technology.
[||] City Unversity of Hong Kong.

10.1021/jp037658u CCC: $27.50

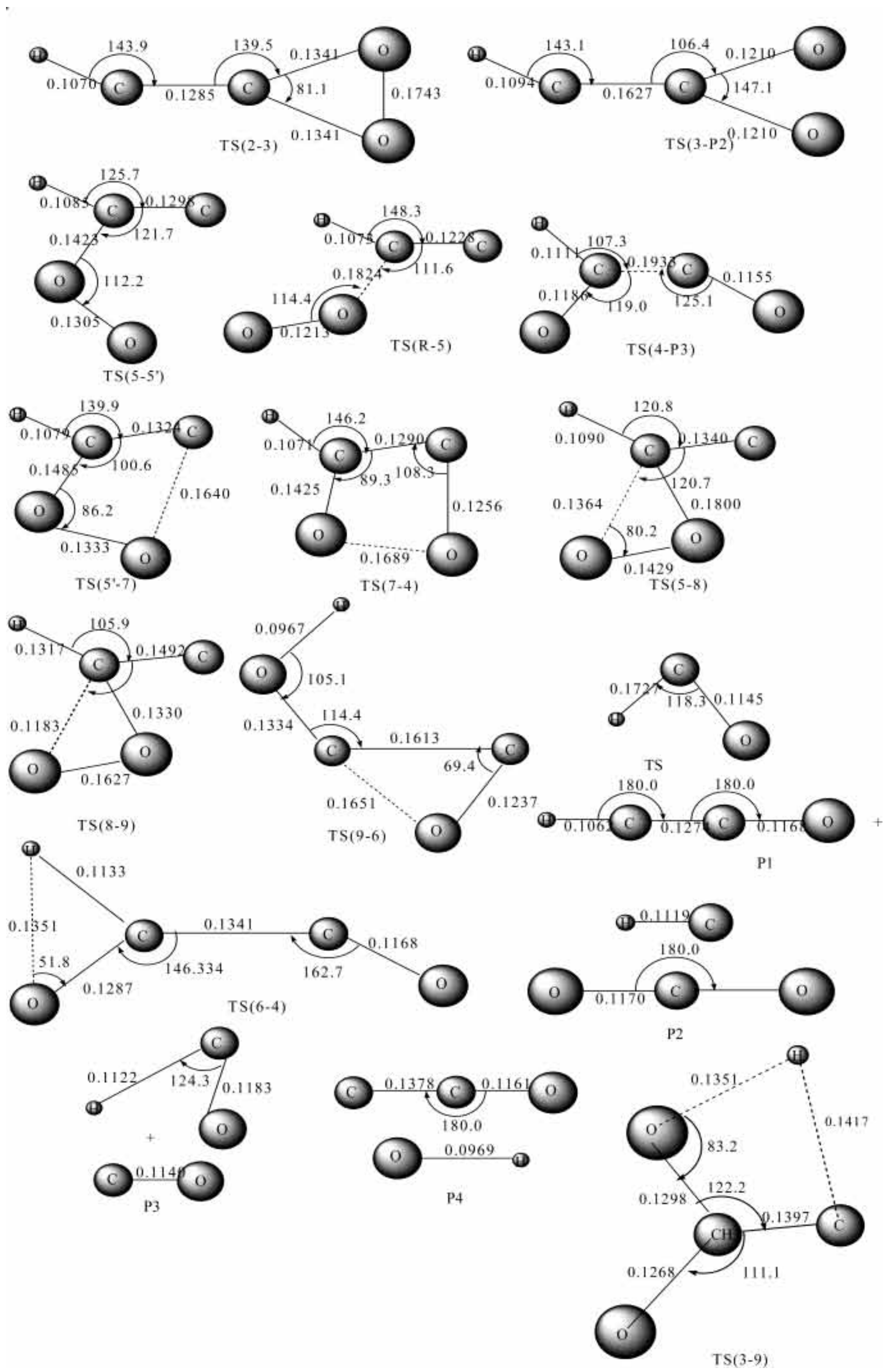

Figure 1. Optimized geometries of the various reactants, intermediates, transition states, and products at the MP2/6-311++G(d,p) level. Bond lengths in nanometers and angles in degrees.

step of reaction of C_2H with O_2. M1 is produced directly by reactants with an oxygen atom of the O_2 molecule attacking the carbon atom not connected to the hydrogen atom of the CCH group, and the process has no activation energy. For another intermediate, M5, if it is produced by reactants, it has to go over the transition states, TS(R-5), so at room temperature the reaction of C_2H and molecular oxygen tends to produce M1. Note that M5 can also be obtained if the reaction could supply energy enough to go over TS(R-5) under a higher temperature condition. Beginning with the intermediates, M1 and M5, there are many reaction pathways, so the reaction mechanism of C_2H with O_2 is very intricate.

As to the pathway M1 → TS(1−2) → M2 → TS(2−3) → M3 → TS(3−P2) → P2(CH + CO_2), this process is a three-member ring reaction mechanism. The COO in TS(1−2) forms a three-member ring during M1 → M2 isomerization. Then, the three-member ring of M2 opens and forms another isomer M3 by the lengthening of the OO bond and cleaving. Finally, M3 can go over a barrier, TS(3−P2), to dissociate, and obtains the products CH radical and CO_2 molecule. Our study finds that the isomerization of M3 can get another intermediate M9 through the transition state TS(3−9), this isomerization activation energy barrier is 18.7 kcal/mol. Comparing the activation energy of the two pathways: M3 → TS(3−P2) → P2(CH + CO_2) and M3 → TS(3−9) → M9, one can find the pathway M3 → TS(3−9) → M9 is more difficult than the pathway M3 → TS(3−P2) → P2(CH + CO_2). Different from M2, M1 can decompose and yield P1(HCCO + H) directly through transition states, TS(1−P1). From Figure 1, the structure of TS(1−P1) shows the dissociation process distinctly.

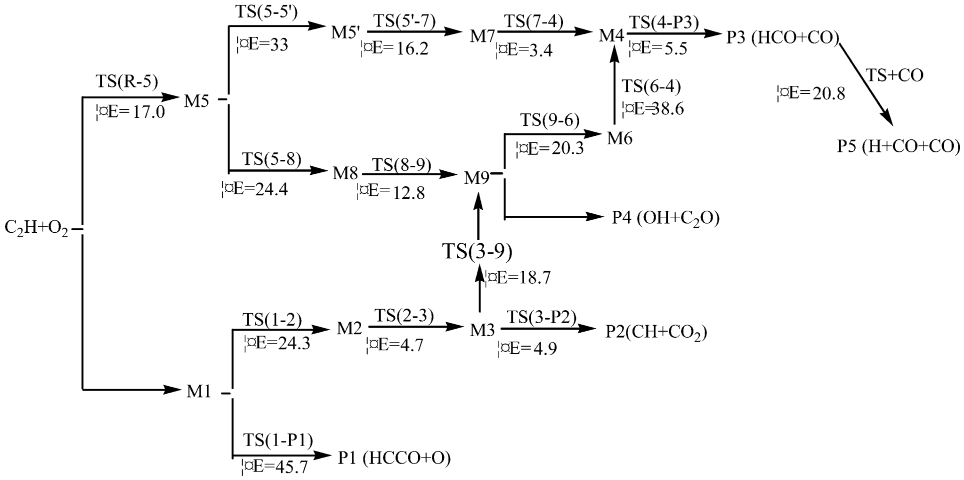

Figure 2. Reaction mechanism and activation energies (kcal/mol) of the reaction of C_2H with O_2.

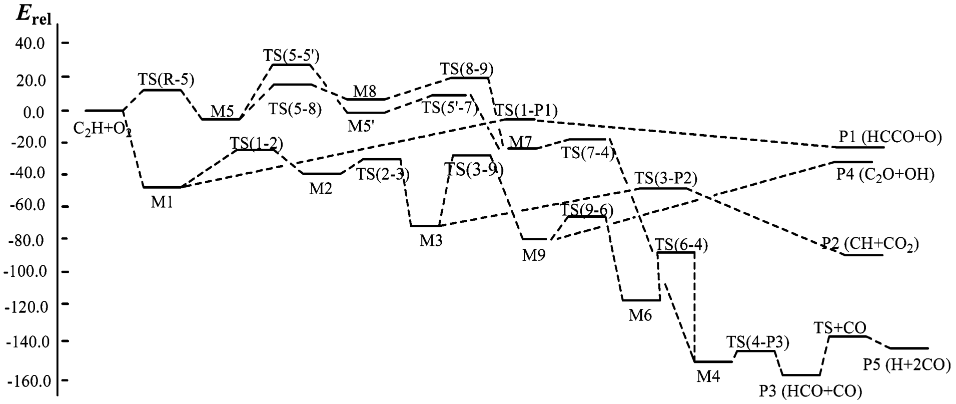

Figure 3. Schematic map of energy levels for the $C_2H + O_2$ reactions. Relative energies are in kilocalories per mole.

If an oxygen atom of O_2 molecule attacks the carbon atom connecting the hydrogen atom with high energy, the reaction may produce the intermediate, M5. Beginning with M5, there are three reaction pathways: M5 → TS(5−5′) → M5′ → TS(5′−7) → M7 → TS(7−4) → M4 → TS(4−P3) → P3(HCO + CO) → TS + CO → P5(H + CO + CO); M5 → TS(5−8) → M8 → TS(8−9) → M9 → P4(OH + C_2O); and M5 → TS(5−8) → M8 → TS(8−9) → M9 → TS(9−6) → M6 → TS(6−4) → M4 → TS(4−P3) → P3(HCO + CO) → TS + CO → P5(H + CO + CO). Among them, the first reaction pathway is a four-member ring reaction mechanism, for CCOO in TS(5′−7) forms a four-member ring during the M5′ → M7 isomerization. M7 can be isomerized to form a more stable intermediate M4, by the opening of the four-member ring. Then the stable intermediate M4 dissociates and yields the HCO radical and CO molecule passing the transition state TS(4−P3). The HCO radical will further dissociate to produce the H atom and CO molecule if with sufficient internal energy. The other two reaction pathways are a three-member ring reaction mechanism. The carbon atom connecting with hydrogen and the two oxygen atoms in TS(5−8) form a three-member ring during the M5−M8 reaction process. M8 can form M9 by the opening of the three-member ring. Beginning with the intermediate M9, there are two channels. One is to form the isomer M6 by an oxygen atom shift. Then M6 can further isomerize to form the more stable intermediate M4, passing a transition state, TS(6−4). The other is to dissociate and yield the products OH and CCO radicals directly.

From the above analysis, we can make the following conclusions: there are two parallel reactions beginning with M1 and three parallel reactions beginning with M5, so the competition reaction mechanism is established for the different products. At the same time, during the reaction process, isomerization among different intermediates will decide the ingredient of different intermediates, and the intermediate M1−M9 will decide the yield of the products. Figures 2 and 3 describe the reaction mechanism of each reaction pathway. It can be seen from these figures that the length of the O−O bond is 0.1224 nm, and the C−O bond length of CO is 0.1140 nm and the C−O bond length of CO_2 is 0.1170 nm. all these bond lengths are close to the data in the literature (0.120 741 ± 0.000 02, 0.1128, and 0.1165 nm [21]). These results indicate the optimizations we have done are accurate and credible.

The above information is the analysis of the reaction mechanism of C_2H with O_2. All intermediates and transition states are confirmed through harmonic vibrational frequency analysis. The eigenvalues of the force constant matrix for all intermediates are positive, and each transition state has and only has a negative eigenvalue. The intrinsic reaction coordinate (IRC) method was used to track minimum energy paths from transition structures to the corresponding local minima, which further confirms the intermediates and transition states.

Theoretical Calculations on Activation Energy and Reaction Heat. On the basis of optimized geometries at the MP2/6-311++G(d.p) level, we used the QCISD(T) method to compute the single stationary points of the reaction of C_2H with O_2 and obtain the relative energy of each species consequently. Table 1 lists MP2, B3LYP, and QCISD(T) energy parameters (including zero-point energy) and relative energy E_{rel} of stationary points on the potential energy surface. On the basis of the relative energies in Table 1, we get the activation energy (kcal/mol) of each reaction pathway (see Figures 2 and 3). Several

TABLE 1: Energies (Corrected by Zero-Point Energies (au)) and Relative Energies (kcal/mol) of Various Species, Computed with Different Methods[a]

species	MP2 6-31G(d)		MP2 6-311++G(d,p)		B3LYP 6-311++G(d,p)		QCISD(T) 6-311++G(d,p)		E_{exp}
	E_{rel}	E	E_{rel}	E	E	E_{rel}	E	E_{rel}	
R(HCC + O_2)	.337 654	0.00	.418 720	0.00	.922 743	0.00	.469 305	0.0	
M1	.390 412	−33.1	.467 865	−30.9	**.062 151**	−87.5	.544 951	−47.4	
TS(1−P1)	.329 854	−4.9	.408 613	−6.4	.942 476	−12.4	.472 080	−1.7	
P1(HCCO + O)	.398 436	−38.2	.478 855	−37.8	**.003 123**	−50.5	.529 441	−37.7	−33
TS(1−2)	.351 368	−8.6	.421 436	−1.7	**.030 286**	−67.5	.506 071	−23.1	
M2	.352 985	−9.6	.464 155	−28.5	**.049 574**	−79.6	.537 421	−42.7	
TS(2−3)	.310 017	17.3	.409 554	−5.8	**.001 078**	−49.2	.529 923	−38.0	
M3	.509 901	−108.1	.503 510	−53.2	**.227 988**	−191.7	.591 897	−76.9	
TS(3−P2)	.392 382	−34.4	.498 181	−49.9	**.110 339**	−117.8	.584 039	−72.0	
P2(CH + CO_2)	.471 334	−83.9	.553 941	−84.9	**.122 904**	−125.7	.614 517	−91.1	−87
TS(R−5)	.246 213	57.4	.296 418	76.8	.904 449	11.5	.442 272	17.0	
M5	.341 878	−2.6	.380 130	24.2	.992 227	−43.6	.475 612	−4.0	
TS(5−5′)	.278 401	37.2	.326 345	58.0	.987 629	−40.7	.423 061	29.0	
M5′	.375 660	−23.9	.384 221	21.7	.990 277	−42.4	.475 067	−3.6	
TS(5−8)	.310 376	17.1	.334 793	52.7	.955 624	−20.6	.436 708	20.4	
M8	.356 206	−11.6	.379 524	24.6	.968 161	−28.5	.460 916	5.3	
TS(8−9)	.303 023	21.7	.340 245	49.3	.929 161	−4.0	.440 436	18.1	
M9	.458 766	−76.0	.542 842	−77.9	**.128 299**	−129.1	.616 133	−92.1	
P4(OH + C_2O)	.391 682	−33.9	.473 178	−34.2	**.010 411**	−55.0	.534 541	−40.9	−36
TS(5′−7)	.256 546	50.9	.356 397	39.1	.968 277	−28.6	.449 250	12.6	
M7	.331 433	−3.9	.428 243	−6.0	**.027 944**	−66.0	.515 628	−29.1	
TS(7−4)	.317 718	12.5	.390 658	17.6	**.026 386**	−65.1	.510 268	−25.7	
M4	.556 297	−137.3	.637 721	−137.5	**.228 012**	−191.7	.710 613	−151.4	
TS(4−P3)	.528 332	−119.7	.636 181	−136.5	**.212 359**	−181.8	.701 870	−145.9	
P3(HCO + CO)	.572 275	−147.3	.655 332	−148.6	**.222 387**	−188.1	.719 694	−157.5	−151
TS + CO	.558 827	−138.8	.633 324	−134.7	**.188 467**	−166.8	.687 182	−136.7	
P5(H + 2CO)	.568 687	−156.5	.646 418	−140.9	**.188 865**	−167.1	.694 628	−141.3	−136
TS(6−4)	.429 345	−57.6	.543 067	−78.1	**.130 565**	−130.5	.610 651	−88.7	
M6	.487 841	−94.3	.601 289	−114.6	**.188 305**	−166.7	.672 193	−127.3	
TS(9−6)	.397 219	−37.4	.507 758	−55.9	**.090 763**	−105.5	.583 844	−71.8	
TS(3−9)	.391 710	−33.9	.475 782	−35.9	**.093 241**	−106.9	.562 835	−58.6	

[a] Numbers before the decimal point in the total energies were omitted (−226 in all cases except the numbers in bold where it is −227).

theoretical levels are selected to calculate all the stationary points of the reaction of C_2H with O_2. Comparing reaction heats of all products of the reactions in Table 1, one can see that the reaction heats of all products calculated at the MP2/6-311++G(d,p) level are closer to the experimental values than those obtained at the MP2/6-31G(d) level. From Table 1, it is clear that the results calculated at the B3LYP/6-311++G(d,p) level are not very good and the results calculated both at the MP2/6-311++G(d,p) level and at the QCISD(T)/6-311++G(d,p) level are closer to the experimental values. So in the following discussion, we chose the results calculated at the QCISD(T)/6-311++G(d,p) level to analyze the change of energies along the pathways and to calculate the activation energy.

The reaction of C_2H with O_2 can produce directly intermediate M1, which is formed by an oxygen atom interacting with the carbon atom without the hydrogen atom in group HCC; the reaction has no activation energy. The products, HCCO and O, are produced by the direct decomposition of M1, and the splitting needs a high activation energy (45.7 kcal/mol). Another reaction pathway beginning with M1 is M1 → TS(1−2) → M2 → TS(2−3) → M3 → TS(3−P2) → P2(CH + CO_2); during the reaction process the three-member ring M2 is formed, so this feasible reaction pathway is a three-member ring reaction mechanism and the controlling step is M1 → TS(1−2) → M2. Its reaction activation energy is 24.3 kcal/mol, which is also the activation energy of the whole reaction pathway. From the energy parameters and relative energy data in Table 1, we can see that the energies of all stabilization states and transition states in the two channels beginning with M1 are lower than those of reactants, so it is impossible to produce the two kinds of products at room temperature. Comparing these two reaction pathways, we can see, beginning with M1, the reaction tends to a three-member ring reaction mechanism; that is, it produces CH and CO_2 more easily.

Intermediate M5 is also produced at the first step of the reaction of C_2H with O_2. This step expects the energy ∼17 kcal/mol. Therefore, reactants can produce the intermediate M5, only possibly at higher temperatures. M5 can produce M5′ passing by TS(5−5′), which then produces a four-member ring, M7, passing by TS(5′−7), so the pathway M5 → TS(5−5′) → M5′ → TS(5′−7) → M7 → TS(7−4) → M4 → TS(4−P3) → P3(HCO + CO) is afour-member ring reaction mechanism. The reaction-controlling step of the channel is M5 → TS(5−5′) → M5′, and its reaction barrier is 33.0 kcal/mol. The products, P3(HCO + CO), can continuously decompose to produce P5(H + CO + CO). With further dissociation the energy 20.8 kcal/mol would be expected. M5 can be isomerized to form a three-member ring M8, and then M8 opens the ring to isomerize forming M9. During the process of reaction, M9 decomposes to form CCO and OH, without the energy barrier. This step requires high energy (51.2 kcal/mol), although it has no activation energy. It is a controlling step of the whole reaction pathway. Comparing these two reaction pathways, we can make a conclusion that the reaction of C_2H with O_2 producing HCO and CO is much easier than producing CCO and OH. This is in agreement with the calculation results of Sumathi et al. employing density functional theory, and it is also responsible for not examining out OH in the experiment up to now. Moreover, we also discover a stable structure M6. M9 can form M4 passing M6. M6 is just like a bridge between M9 and M4. This is the third reaction pathway beginning with M5, that is, M5 → TS(5−8) → M8 → TS(8−9) → M9 → P4(OH +

$C_2O) \rightarrow TS(9-6) \rightarrow M6 \rightarrow TS(6-4) \rightarrow M4 \rightarrow TS(4-P3) \rightarrow P3(HCO + CO) \rightarrow TS + CO \rightarrow P5$. The controlling step of this pathway is $M6 \rightarrow TS(6-4) \rightarrow M4$. Its reaction activation energy is 38.6 kcal/mol. Comparing the energies of all intermediates in the three channels beginning with M5, we find that the energy of M4 is the smallest. So the reaction producing P3(HCO + CO) is relatively easy.

By comparing the five above-mentioned reaction pathways of C_2H with O_2, we find that there is no energy barrier in the formation of M1, and however, for the formation of M5 the activation energy of 17.0 kcal/mol is expected. So at room temperature the main channel of this reaction is $C_2H + O \rightarrow M1 \rightarrow TS(1-2) \rightarrow M2 \rightarrow TS(2-3) \rightarrow M3 \rightarrow TS(3-P2) \rightarrow P2(CH + CO_2)$.

In this study, we also obtained the reaction heats of different products (CO + HCO, 2CO + H, CH + CO_2, and HCCO + O), which are −157.5, 141.3, −91.1, −40.9, and −37.7 kcal/mol, respectively, and all of them are close to the data in the literature in the preface mentioned. This indicates the results that we have obtained are credible.

4. Conclusion

The ab initio MP2 method with the 6-311++G(d,p) basis set has been used to study the complicated microscopic reaction mechanism of C_2H radical and oxygen molecule, and the QCISD(T)/6-311++G(d,p) method has been used to compute the single-point energy of stationary points. Comparing with the experimental values, reliable activation energies of the five different reaction pathways and theoretical reaction heats of different products are obtained. At the same time, results obtained at the MP2/6-31G(d) level and at the B3LYP/6-311++G(d,p) level are also discussed. Our results clearly show that, at room temperature, the main reaction pathway of C_2H and oxygen is $C_2H + O_2 \rightarrow M1 \rightarrow TS(1-2) \rightarrow M2 \rightarrow TS(2-3) \rightarrow M3 \rightarrow TS(3-P2) \rightarrow CH + CO_2$.

References and Notes

(1) Ronne, H.; Homann, K. H.; Wager, H. Hg. *Symp. (Int.) Combust. [Proc.].* **1965**, *10*, 503.

(2) Frenklach, M.; Clary, D. W.; Gardiner, W. C.; Stein, S. E. *Symp. (Int.) Combust. [Proc.].* **1984**, *20*, 887.

(3) Shaub, W. M.; Bauer, S. H. *Combust. Flame* **1978**, *32*, 35.

(4) Boullart, W.; Devriendt, K.; Borm, R.; Peeter, J. *J. Phys. Chem.* **1996**, *100*, 998.

(5) Vakhtin, A. B.; Smith, I. W. M.; Leone, S. R.; Heard, D. E. *Chem. Phys. Lett.* **2001**, *348*, 21.

(6) Look, H. V.; Peeters, J. *J. Phys. Chem.* **1995**, *99*, 16284.

(7) Lange, W.; Wagner, H. G. *Ber. Bunsen-Ges. Phys. Chem.* **1975**, *79*, 165.

(8) Renlund, A. M.; Shokoohi, F.; Reisler, H.; Wittig, C. *Chem. Phys. Lett.* **1981**, *84*, 293.

(9) Renlund, A. M.; Shokoohi, F.; Reisler, H.; Wittig, C. *J. Phys. Chem.* **1982**, *86*, 4165.

(10) Devriendt, K.; Van Look, H.; Ceursters, B.; Peeters, J. *Chem. Phys. Lett.* **1996**, *261*, 450.

(11) Laufer, A. H.; Lechleider, R. *J. Phys. Chem.* **1984**, *88*, 66.

(12) Stuphens, J. W.; Hall, J. L.; Sodka, H.; Yan, W. B.; Curl, R. F.; Glass, G. P. *J. Phys. Chem.* **1987**, *91*, 5740.

(13) Lander, D. R.; Unfried, K. G.; Stephens, J. W.; Glass, G. P.; Curl, R. F. *J. Phys. Chem.* **1989**, *93*, 4109.

(14) Lander, D. R.; Unfried, K. G.; Glass, G. P.; Curl, R. F. *J. Phys. Chem.* **1990**, *94*, 7759.

(15) Pedersen, J. O. P.; Opansky, B. J.; Leone, S. R. *J. Phys. Chem.* **1993**, *97*, 6822.

(16) Opansky, B. J.; Seakins, P. W.; Pedersen, J. O. P.; Leone, S. R. *J. Phys. Chem.* **1993**, *97*, 8583.

(17) Van Look, H.; Peeters, J. *J. Phys. Chem.* **1995**, *99*, 16284.

(18) Thiesemann, H.; Taatjes, C. A. *Chem. Phys. Lett.* **1997**, *270*, 580.

(19) Sumathi, R.; Peeter, J.; Nguyen, M. T. *Chem. Phys. Lett.* **1998**, *287*, 109.

(20) Frisch, M. J.; Trucks, G. W.; Head Gordon, M.; Gill, P. M. W.; Wong, M. W.; Foresman, J. B.; Johnson, B. G.; Schlegel, H. B.; Robb, M. A.; Replogle, E. S.; Gompert, R. J.; Andres, L.; Raghavachari, K.; Binkley, J. S.; Gonzalez, C.; Martin, R. J.; Fox, D. J.; Defrees, B. J.; Baker, J.; Stewart, J. J. P.; Pople, J. A. *Gaussian94*; Gaussian, Inc., Pittsburgh, PA, 1994.

(21) Yao, Y. B.; Xie, T.; Gao, Y. M. *The Manual of Physical Chemistry*, 1st ed.; Shanghai Science and Technology Press: Shanghai, China, 1985.